Scientific paper

Fe_3O_4@SiO_2-NH_2 Nanocomposite as a Robust and Effective Catalyst for the One-pot Synthesis of Polysubstituted Dihydropyridines

Mohammad Ali Ghasemzadeh* and Mohammad Hossein Abdollahi-Basir

Department of Chemistry, Qom Branch, Islamic Azad University, Qom, I. R. Iran
Department of Organic Chemistry, Faculty of Chemistry,

** Corresponding author: E-mail: Ghasemzadeh@qom-iau.ac.ir*

Received: 27-02-2016

Abstract

A practical, simple and efficient method for the synthesis of polysubstituted dihydropyridines was described via multi-component reactions of aldehydes, arylamines, dimethyl acetylenedicarboxylate and malononitrile/ethyl acetoacetate in the presence of Fe_3O_4@SiO_2-NH_2 nanocomposites. The present methodology provides a novel and efficient method for the synthesis of dihydropyridine derivatives with some advantages, such as excellent yields, short reaction times, recoverability and low catalyst loading. The nanomagnetic catalyst could be readily recovered using an external magnet and reused several times without any significant loss in activity. The catalyst was fully characterized by FT-IR, SEM, XRD, EDX and VSM analysis.

Keywords: Fe_3O_4@SiO_2-NH_2, magnetite, multi-component reaction, nanocatalyst, dihydropyridine.

1. Introduction

Substituted dihydropyridone derivatives are an important class of nitrogen heterocyclic compounds due to a variety of biological and pharmacological activities[1] such as: antihypertension,[2] antioxidant,[3,4] anticancer[5] and antitumor activity.[6] However, there are many methods for the synthesis of dihydropyridines. Among various dihydropyridine structures, some of them have medicinal properties such as: nicardipine **1** and nifedipine **2**,[7] isradipine **3** and niguldipine **4**,[8] which exhibit dihydropyridine moiety (Figure 1).

Consequently, synthesis of highly functionalized dihydropyridine derivatives, with the aim of developing new drug molecules has been an active area of research. Recently, much attention has been paid to the development of new methodologies for the preparation of dihydropyridines. The main synthetic routes for the preparation of substituted dihydropyridines are Hantzsch method via the cyclocondensation of an aldehyde, β-ketoester and ammonia,[9] regioselective [4+2] cycloaddition of 1-aryl-4-phenyl-1-azadienes and allenic esters for the synthesis of *N*-aryl-1,4-DHPs,[10] and a multi-component reaction of alkyl amines, ethyl propiolate, and benzal-

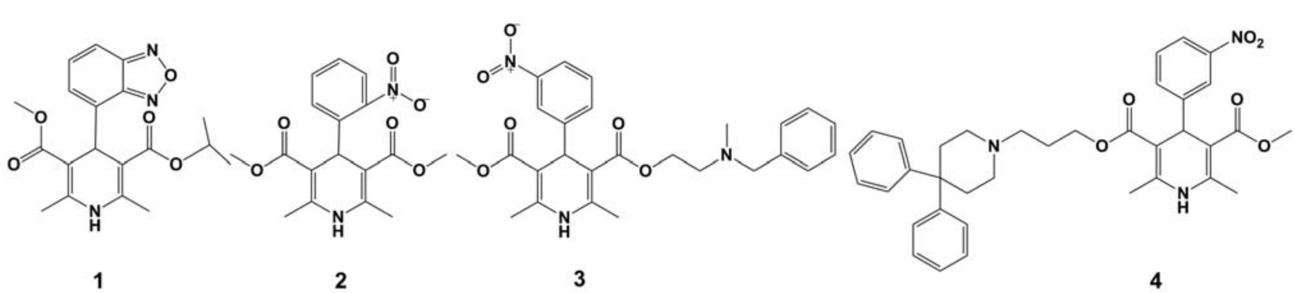

Figure 1. Some biologically important dihydropyridine derivatives

dehydes for the construction of *N*-alkyl-1,4-DHPs,[11] and other methods.

Recently, a few methods have been reported for the syntheses of polysubstituted dihydropyridines via four-component reactions of aldehydes, arylamines, acetylenedicarboxylates and malononitrile/ethyl acetoacetate using Et_3N,[12] NaOH,[13] $(NH_4)_2HPO_4$.[14]

In the modern science, one of the growing and important fields is nanotechnology. Because of different physical and chemical properties of nano-sized catalysts compared to bulk material, they attract interests in different researcher areas.[15] Since the particles are small in size, the surface area exposed to the reactant is maximized so allowing more reactions to occur at the same time, hence the process is accelerated.[16]

Magnetic nanoparticles show a great potential as catalysts because of their large surface area and the large ratio of atoms available at the surface to perform the chemical transformation of substrates.[17,18] However, the bare Fe_3O_4 nanoparticles have high reactivity and easily undergo degradation upon direct exposure to certain environments, leading to poor stability and dispersity. Therefore, the surface of magnetic nanoparticles should be modified to improve the dispersity and biocompatibility, which could significantly facilitate its utilization.

Fe_3O_4@SiO_2-NH_2 nanocomposites are one of the most important supported magnetite nanostructures which have received great attention due to their significant properties and potential applications in various fields.[19] This kind of catalyst is eco-friendly, non-toxic, non-volatile and can be recycled several times without loss of activity in the reaction. The use of these nanoparticles follows the principles of green chemistry.

Recently, functionalized Fe_3O_4 nanocatalysts were applied as a robust and effective catalyst in many organic reactions, such as: Knoevenagel condensation and Michael addition,[20] Suzuki and Heck cross-coupling,[21] asymmetric aldol reaction,[22] Suzuki coupling,[23] asymmetric hydrogenation of aromatic ketones,[24] acetalization reaction,[25] reduction of nitro aromatic compounds,[26] cyanosilylation of carbonyl compounds,[27] Henry reaction,[28] enantioselective direct-addition of terminal alkynes to imines.[29]

In continuation of the progress of the synthetic approach to the synthesis of heterocyclic compounds using reusable nanocatalysts and multi-component reactions,[30–34] herein we report a simple, efficient, mild and practical method for the synthesis of polysubstituted dihydropyridines via a four-component coupling reaction in the presence of Fe_3O_4@SiO_2-NH_2 nanocomposite as a green and environmentally benign nanocatalyst in ethanol as solvent at room temperature (Scheme 1).

2. Results and Discussion

The chemical purity of the samples as well as their stoichiometry was tested by energy dispersive X-ray spectroscopy (EDX) studies. The EDX spectrum given in Figure 2a shows the presence of Fe and O as the only elementary components of Fe_3O_4 NPs. EDX spectrum of Fe_3O_4@SiO_2 in Figure 2b shows the elemental composition of core–shell nanocomposite to be Fe, Si and O. EDX

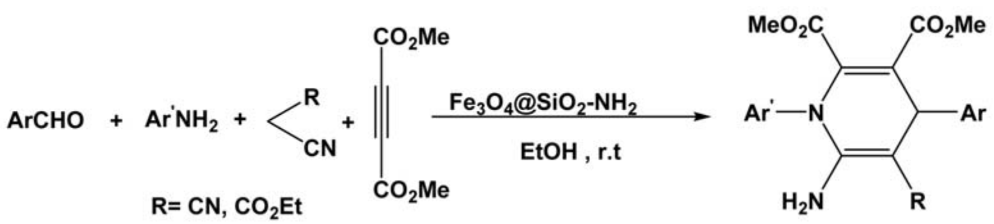

Scheme 1. Synthesis of polysubstituted dihydropyridines catalyzed by Fe_3O_4@SiO_2-NH_2 nanocomposite

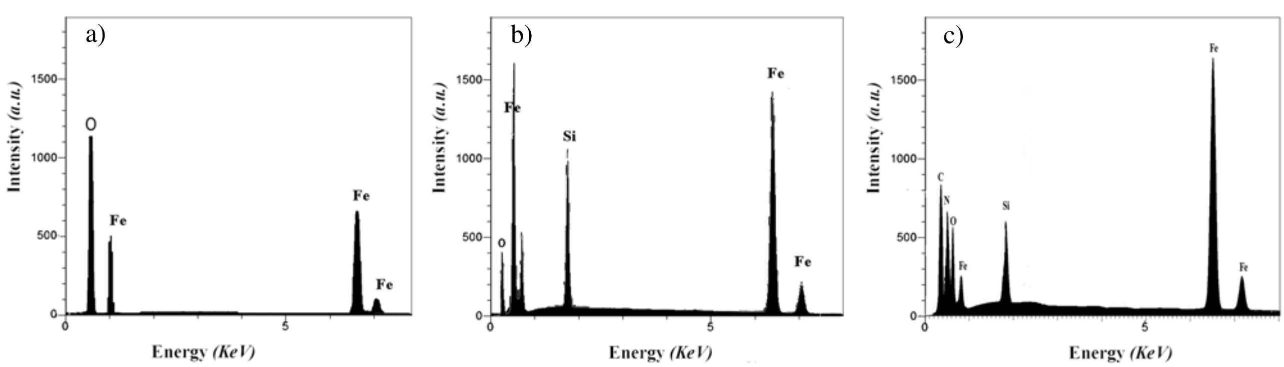

Figure 2. The EDX spectra of Fe_3O_4 (a), Fe_3O_4@SiO_2 (b) and Fe_3O_4@SiO_2@-NH_2 (c)

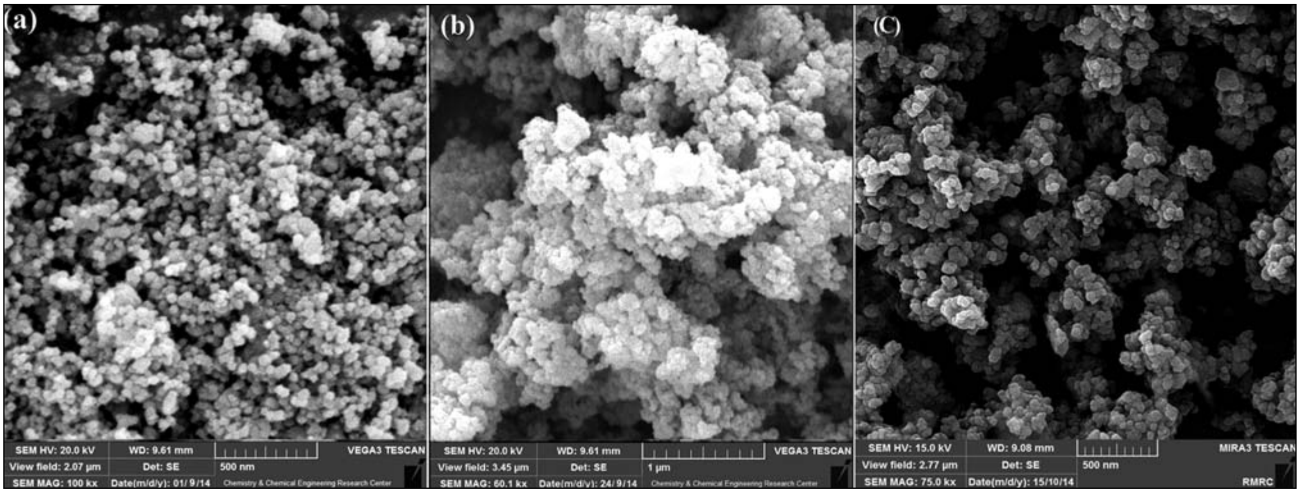

Figure 3. The SEM images of Fe_3O_4 (a), Fe_3O_4@SiO_2 (b) and Fe_3O_4@SiO_2-NH_2 (c)

spectrum of Fe_3O_4@SiO_2-NH_2 in Figure 2c shows the elemental composition of amino-functionalization silica-coated magnetite nanocomposite with core–shell structure to be Fe, Si, C, O and N.

Scanning electron microscopy (SEM) images of the prepared nanostructures are shown in Figure 3. Figure 3a shows that the Fe_3O_4 nanoparticles are cubic in shape with an average size about 15 nm. Figure 3b (Fe_3O_4@SiO_2) and Figure 3c (Fe_3O_4@SiO_2-NH_2) show that both are apparently of similar shape, but approximate size of amino-functionalization silica-coated magnetite nanocomposite is more than *r* of the Fe_3O_4@SiO_2 core–shell nanocomposite.

The structures of Fe_3O_4 (a), Fe_3O_4@SiO_2 (b) and Fe_3O_4@SiO_2-NH_2 (c) were analyzed by X-ray diffraction (XRD) spectroscopy (Figure 4). XRD diagram of the bare Fe_3O_4 NPs displayed patterns consistent with the patterns of spinel ferrites (Figure 4a). The same peaks were observed in both of the Fe_3O_4@SiO_2 (Figure 4b) and Fe_3O_4@SiO_2-NH_2 (Figure 4c) XRD patterns, indicating retention of the crystalline spinel ferrite core structure during the coating process. The average MNPs core diame-

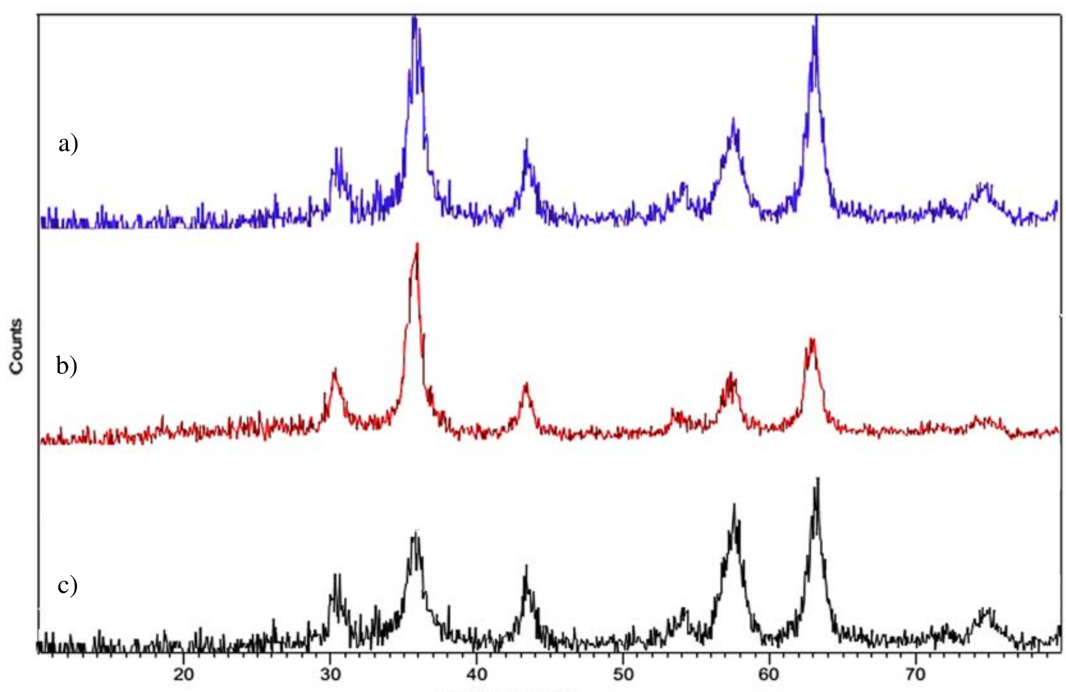

Figure 4. X-ray diffraction for Fe_3O_4 (a), Fe_3O_4@SiO_2 (b) and Fe_3O_4@SiO_2-NH_2 (c)

ters of Fe_3O_4, $Fe_3O_4@SiO_2$ and $Fe_3O_4@SiO_2$-NH_2 were calculated to be about 18, 25 and 40 nm, respectively, from the XRD results by Scherrer's equation, ($D = K\lambda/\beta\cos\theta$), where β FWHM (full-width at half-maximum or half-width) is in radian and θ is the position of the maximum of diffraction peak, K is the so-called shape factor, which usually takes a value of about 0.9, and λ is the X-ray wavelength (1.5406 Å for Cu Kα).

The FT-IR spectra of Fe_3O_4, $Fe_3O_4@SiO_2$ and $Fe_3O_4@SiO_2$-NH_2 nanostructures are shown in Figure 5. For the bare magnetic nanoparticle (Figure 5a) the vibration band at 567 cm^{-1} is the typical IR absorbance induced by structure Fe–O vibration. In the case of $Fe_3O_4@SiO_2$ nanocomposite (Figure 5b), the band at 1072 cm^{-1} is corresponding to Si–O–Si antisymmetric stretching vibrations, being indicative of the existence of SiO_2 on the nanoparticles. $Fe_3O_4@SiO_2$-NH_2 can be ascribed to the stretching and deformation vibrations of SiO_2, reflecting the coating of amino group on the $Fe_3O_4@SiO_2$ core–shell nanocomposite surfaces. Successful aminopropyl functionalization of the silica layer on $Fe_3O_4@SiO_2$ was also evidenced by the absorption at 1478 cm^{-1} attributed to bending vibrations of amino groups. The absorption peaks in the region 2800–3025 cm^{-1} were associated with the stretching vibration of methylene groups of $Fe_3O_4@SiO_2$-NH_2 (Figure 5c). The results verified the formation of a silica shell on the Fe_3O_4 surface and the amino-functionalization of the silica shell.

The magnetic properties of the uncoated magnetic iron oxide (Fe_3O_4), $Fe_3O_4@SiO_2$, and $Fe_3O_4@SiO_2$-NH_2 were measured by vibrating sample magnetometer, VSM, at room temperature (Figure 6). The hysteresis loops that are characteristic of superparamagnetic behavior can be clearly observed for all the nanostructures. Superparamagnetism is the responsiveness to an applied magnetic field without retaining any magnetism after removal of the applied magnetic field. From M versus H curves, the saturation magnetization value (Ms) of uncoated Fe_3O_4 NPs was found to be 47.12 emu g^{-1}. For $Fe_3O_4@SiO_2$ and $Fe_3O_4@SiO_2$-NH_2, the magnetizations obtained at the same field were 41.23 and 32.42 emu g^{-1}, respectively, lower than that of uncoated Fe_3O_4. These results indicated that the magnetization of Fe_3O_4 decreased considerably with the increase of SiO_2 and aminopropyl groups. This is mainly attributed to the existence of nonmagnetic materials on the surface of the nanoparticles.

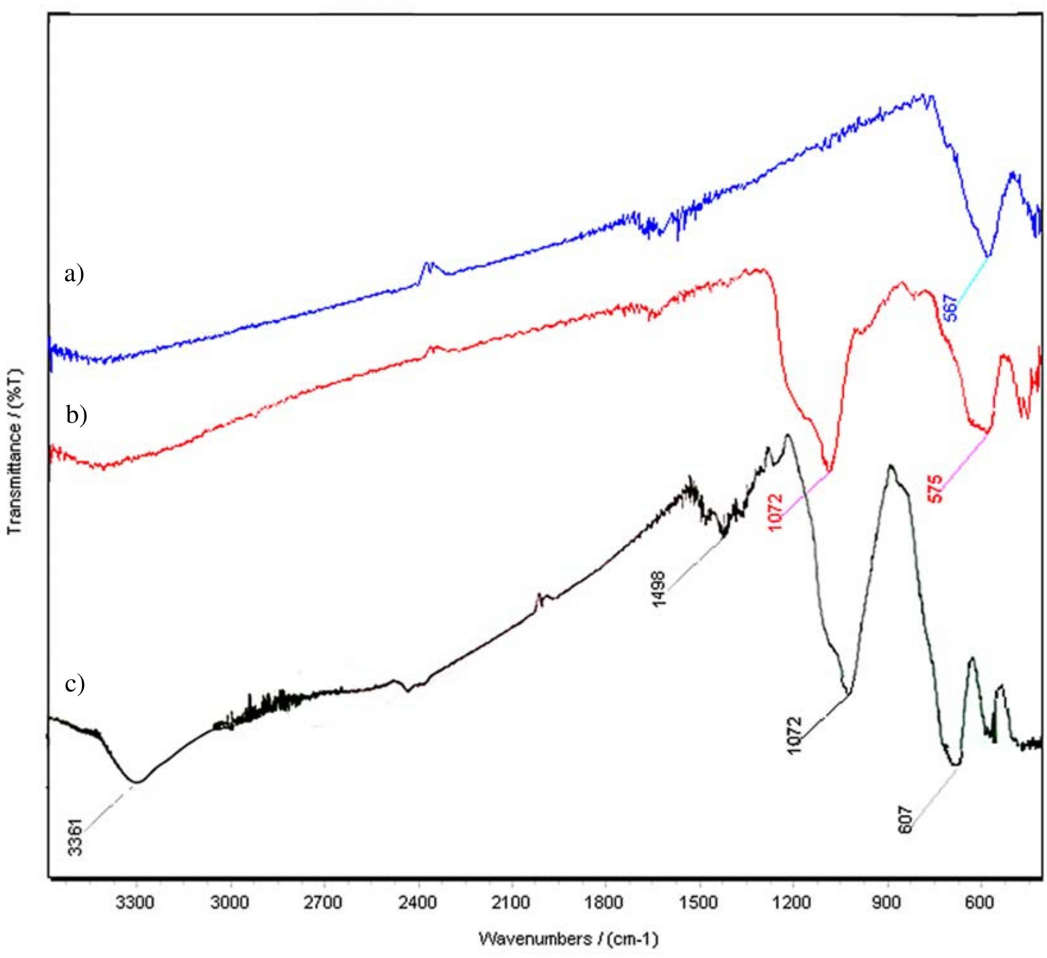

Figure 5. The comparative FT-IR spectra of Fe_3O_4 (a), $Fe_3O_4@SiO_2$ (b) and $Fe_3O_4@SiO_2$-NH_2 (c)

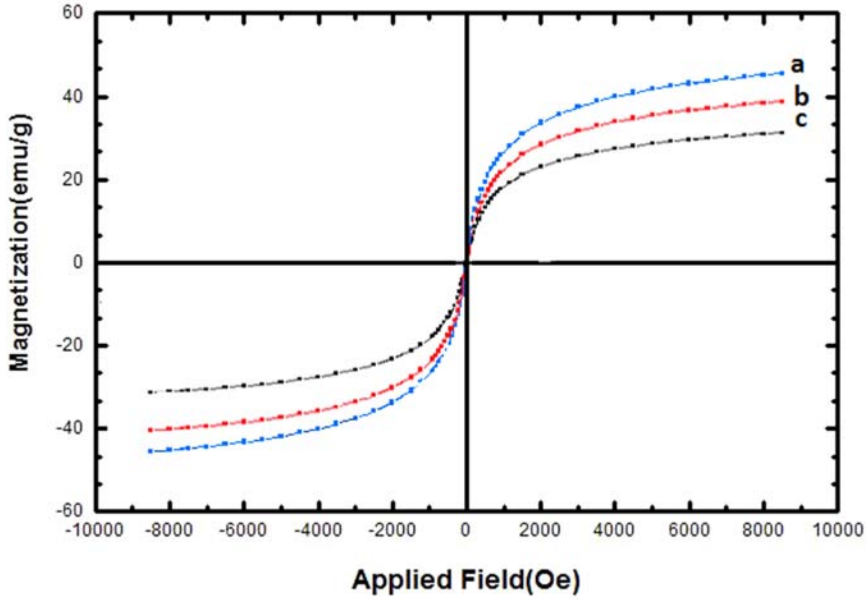

Figure 6. VSM magnetization curves of Fe_3O_4 (a), Fe_3O_4@SiO_2 (b) and Fe_3O_4@SiO_2-NH_2 (c)

We decided to optimize the four-component reaction of benzaldehyde, aniline, dimethyl acetylenedicarboxylate and malononitrile as a model study. The reaction conditions were optimized on the base of solvents, catalysts and different temperatures. The product of this model reaction is dimethyl-6-amino-5-cyano-4-(4-cyanophenyl)-1-phenyl-1,4-dihydropyridine-2,3-dicarboxylate (**5a**) (Scheme 2).

Firstly, to obtain the best reaction conditions for the synthesis of polysubstituted dihydropyridine **5a**, the model study was carried out in the presence of various catalytic systems including homogenous and heterogeneous catalysts. As can be seen from Table 1, among the various catalysts, Fe_3O_4@SiO_2-NH_2 core–shell nanostructures were found to be the most effective catalyst for the synthesis of polysubstituted dihydropyridine **5a** at room temperature.

To find the optimized amount of the catalyst, the preparation of dihydropyridine **5a** was carried out using different amounts of Fe_3O_4@SiO_2-NH_2 as the catalyst (0.002, 0.005, 0.01, 0.02, 0.03 g). The best result was obtained by using 0.01 g of Fe_3O_4@SiO_2-NH_2 nanocomposites at room temperature.

In continuation of this research, to select the appropriate solvent, various solvents such as, dichloromethane, DMF, water, toluene and ethanol were used in the model reaction in the presence of Fe_3O_4@SiO_2-NH_2 at room

Table 1. Yields and reaction times for the preparation of 1,4-dihydropyridine **5a** in the presence of various catalysts.[a]

Entry	Catalyst	Time (h)	Yield (%) [b]
1	None	10	–
2	NaOH	7	75
3	Et_3N	8	78
4	pipyridine	10	70
5	CaO NPs	6	78
6	MgO NPs	5.5	75
7	ZnO NPs	12	55
8	Fe_3O_4 NPs	8	66
9	Fe_3O_4@SiO_2	6	72
10	**Fe_3O_4@SiO_2-NH_2**	**4**	**94**

[a] Reaction conditions: benzaldehyde (1 mmol), malononitrile (1 mmol) aniline (1 mmol) and acetylenedicarboxylate (1 mmol) in ethanol (10 mL) at r.t. [b] Isolated yield.

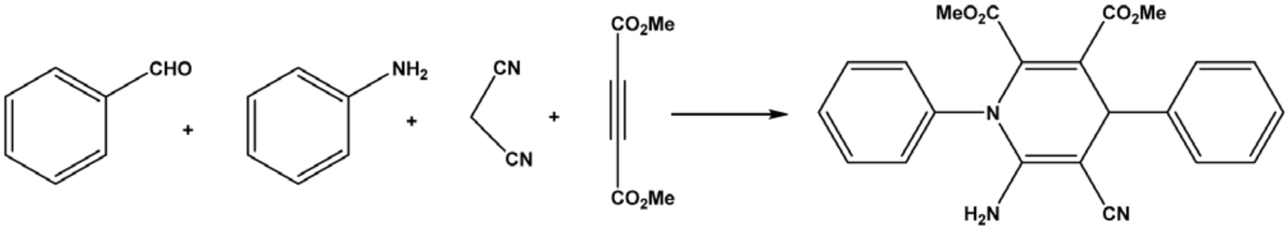

Scheme 2. The model reaction for the synthesis of dihydropyridine **5a**

temperature. As shown in Table 2, we found that ethanol is the most efficient solvent for the synthesis of polysubstituted dihydropyridine **5a**, giving the product in 94% yield (Table 2, entry 6).

Table 2. The effect of solvents/reaction times on the yield of dihydropyridine **5a**

Entry	Solvent	Time (h)	Yield (%)[b]
1	Solvent Free	6	35
2	Dichloromethane	10	52
3	DMF	6	68
4	Water	8	65
5	Toluene	12	45
6	**Ethanol**	**4**	**94**

[a] Reaction conditions: benzaldehyde (1 mmol), malononitrile (1 mmol) aniline (1 mmol) and acetylenedicarboxylate (1 mmol) in various solvents (10 mL) at r.t. in the presence of Fe_3O_4@SiO_2-NH_2 (0.01 g). [b] Isolated yield.

The substrate scope of this protocol for the synthesis of a variety of polysubstituted dihydropyridines was studied next by applying various amines and aldehydes to the reaction (Scheme 1 and Table 3). As shown in Table 3, aniline derivatives, including those bearing electron-donating or electron-withdrawing as well as sterically demanding substituents, reacted very well to afford the desired products **5a–t** in excellent yields over short reaction times. Also, various arylamines with electron-releasing groups such as methoxy and methyl groups reacted in short reaction times and giving products with higher yields than those with electron-withdrawing groups such as NO_2 and Cl.

In addition, aryl aldehydes with electron-withdrawing groups such as NO_2, Cl and Br reacted very smoothly to produce highly functionalized dihydropyridines in relatively short reaction times in comparison with aryl aldehydes bearing electron-donating groups, but sterically hindered aldehydes reacted more slowly compared to unhindered aldehydes.

As the results in Table 3 show, Fe_3O_4@SiO_2-NH_2 proved to be a useful nanomagnetic heterogeneous acid nanocatalyst for green synthesis of polysubstituted dihydropyridines in excellent yields.

A plausible mechanism for the preparation of highly functionalized dihydropyridines using Fe_3O_4@SiO_2-NH_2 NPs is shown in Scheme 4, given on the basis of our experimental results together with some literature data.[12–14]

It is likely that NH_2 groups on the surfaces of nanoparticles act as a Brønsted base and cause the dehydrogenation of substrates. First, the Knoevenagel condensation of malononitrile/ethyl acetoacetate is suggested to give the intermediate **A**. Then, a nucleophilic attack of arlymine to dimethyl acetylenedicarboxylate leads to the formation of intermediate **B**. Michael addition of intermediate **B** to **A** forms the intermediate **C** which undergoes an intramolecular cyclization which is catalyzed by Brønsted basic (–NH_2) functionalized Fe_3O_4 core–shell nanoparticles. In the last step, the intermediate **D** is tautomerized to the product **4**.

Table 3. Yields and reaction times for the preparation of dihydropyridines **5a–t** using Fe_3O_4@SiO_2-NH_2 nanocomposite[a]

Entry	Ar	Ar'	R	Product	Time (h)	Yield (%)[b]	m.p. (°C)	Lit. m.p (°C)
1	H	H	CN	**5a**	4	94	162–164	(161–163)[13]
2	H	4-Me	CN	**5b**	4	96	165–167	(165–167)[13]
3	4-Cl	4-Me	CN	**5c**	3.5	97	184–186	(186–188)[13]
4	4-Br	4-Me	CN	**5d**	3.5	95	186–188	(185–187)[13]
5	3-Cl	4-Me	CN	**5e**	7	90	181–183	(180–182)[13]
6	3-NO_2	4-Me	CN	**5f**	5	90	210–212	(212–214)[13]
7	4-OMe	4-OMe	CN	**5g**	4.5	88	162–163	(159–161)[13]
8	4-Cl	4-Cl	CN	**5h**	4	95	130–132	(130–132)[13]
9	4-OMe	4-Me	CN	**5i**	4	92	167–169	(168–170)[13]
10	3-NO_2	4-OMe	CN	**5j**	4	90	185–187	(184–186)[13]
11	3-NO_2	4-Cl	CN	**5k**	5	86	195–197	(195–197)[13]
12	4-Br	4-Cl	CN	**5l**	4	91	164–166	(163–165)[13]
13	3-NO_2	4-Me	COOEt	**5m**	4.5	88	172–174	–
14	3-NO_2	4-OMe	COOEt	**5n**	4	88	178–180	–
15	4-Cl	H	CN	**5o**	3.5	94	138–140	–
16	4-NO_2	4-Cl	CN	**5p**	4	93	185–187	–
17	4-Cl	3-NO_2	CN	**5q**	5	95	157–159	–
18	4-Me	4-Cl	CN	**5r**	4.5	91	191–193	–
19	4-$CH(CH_3)_2$	4-Cl	CN	**5s**	5	86	195–197	–
20	4-CN	4-Cl	CN	**5t**	4	94	164–166	–

[a] Reaction conditions: aldehyde (1 mmol), malononitrile/ethylcyanoacetate (1 mmol), aromatic amine (1 mmol) and acetylenedicarboxylate (1 mmol) in ethanol (10 mL) for various times in the presence of Fe_3O_4@SiO_2-NH_2. [b] Isolated yields.

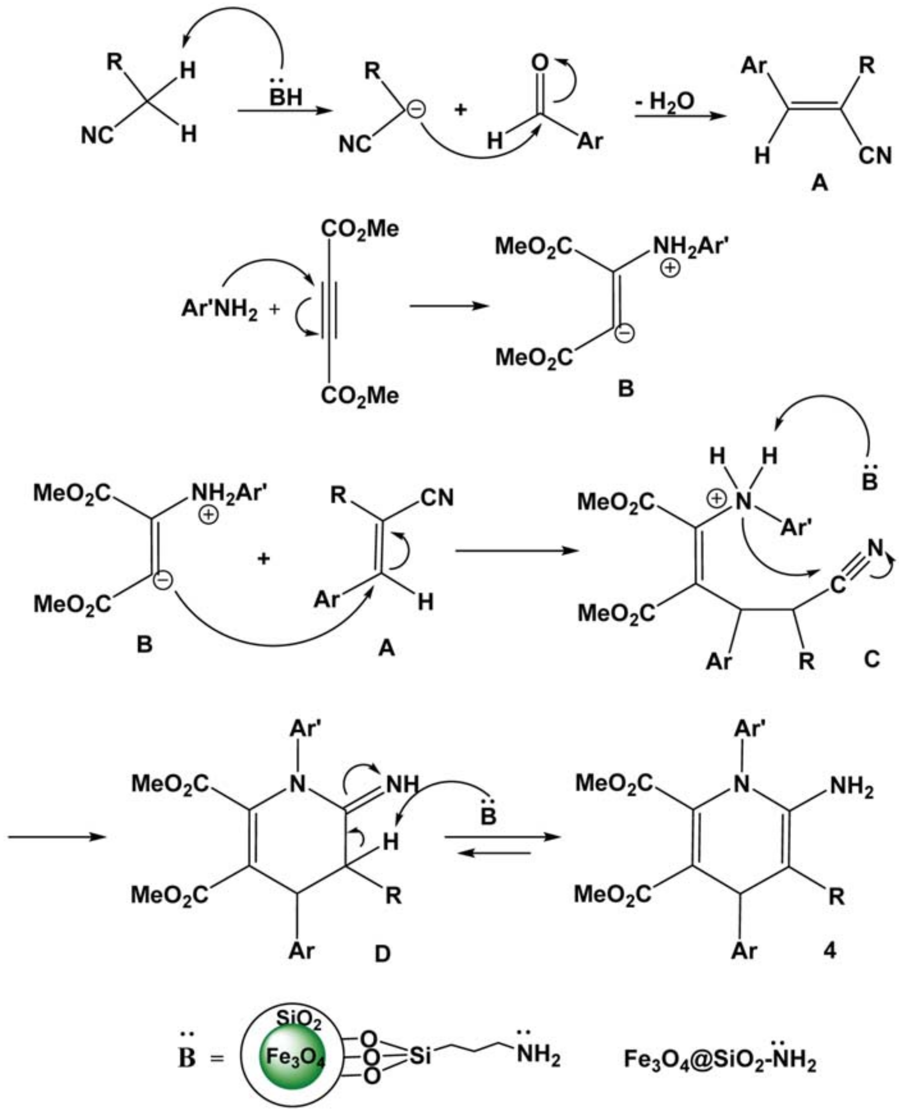

Scheme 3. The proposed mechanism for the synthesis of dihydropyridines by Fe_3O_4@SiO_2-NH_2 NPs

3. Experimental

3. 1. General

Chemicals were purchased from the Sigma-Aldrich and Merck in high purity. All of the materials were of commercial reagent grade and were used without further purification. All melting points are uncorrected and were determined in capillary tube on Boetius melting point microscope. NMR spectra were obtained on a Bruker DRX-400 MHz spectrometer (^1H NMR at 400 Hz, ^{13}C NMR at 100 Hz) with $CDCl_3$ as the solvent, using TMS as an internal standard. Chemical shifts (δ) are given in ppm and coupling constants (*J*) in Hz. FT-IR spectrum was recorded on Magna-IR, spectrometer 550. The elemental analyses (C, H, N) were obtained from a Carlo Erba Model EA 1108 analyzer. Powder X-ray diffraction (XRD) was carried out on a Philips diffractometer of X'pert Company with monochromatic Cu Kα radiation (λ = 1.5406 Å). Microscopic morphology of the products was visualized by SEM (LEO 1455VP). The mass spectra were recorded on a Joel D-30 instrument at an ionization potential of 70 eV. Magnetic properties were obtained on a BHV-55 vibrating sample magnetometer (VSM) made by MDK, I. R. Iran. The compositional analysis was done by energy dispersive analysis of X-ray (EDX, Kevex, Delta Class I).

3. 2. Preparation of Fe_3O_4 Nanoparticles

Fe_3O_4 NPs were prepared according to a procedure previously reported by Hu et al[35] using the chemical co-precipitation method. Typically, $FeCl_3 \cdot 6H_2O$ (2.7 g) and $FeCl_2 \cdot 4H_2O$ (1.0 g) were dissolved in aqueous HCl (100 mL, 1.2 mM) in an ultrasonic bath (30 min). Then, aqueous NaOH (150 mL, 1.25 M) was added under vigorous stirring and a black precipitate was immediately formed. The resulting solution was heated at 80 °C with rapid mechanical stirring under N_2 atmosphere (2 h). The black products were centrifuged, filtered off and washed with deionized water and ethanol several times, and finally dried at 60 °C for 12 h.

3. 3. Preparation of Fe_3O_4@SiO_2 Nanoparticles

Fe_3O_4@SiO_2 core–shell nanoparticles were prepared via modified Stöber sol-gel process.[36] 30 mg as-prepared Fe_3O_4 submicrospheres were ultrasonically dispersed in a solution containing 160 mL ethanol, 40 mL water and 10 mL concentrated ammonia (28 wt%). Then, 0.4 mL TEOS was added dropwise to the solution under sonication, followed by mechanical stirring for 3 h at room temperature. Subsequently, the resulting particles were separated using a magnet and washed with deionized water and ethanol. This step was repeated several times before drying at 60 °C for 12 h.

3. 4. Preparation of Fe_3O_4@SiO_2-NH_2

Fe_3O_4@SiO_2-NH_2 MNPs were prepared according to a previously reported procedure by Jiahong Wang et al.[37] Amino-functionalized Fe_3O_4@SiO_2 nanocomposite was prepared by surface functionalization of Fe_3O_4@SiO_2 nanocomposite using (3-aminopropyl)triethoxysilane (APTES). 2 g of Fe_3O_4@SiO_2 nanocomposite and 50 mL of toluene were added to a 250 mL three-necked flask and then ultrasonically dispersed for 15 min. 4 mL of APTES (Sigma) was then added into the flask, and the mixture was refluxed at 110 °C with continuous stirring for 12 h under a nitrogen flow (40 mL/min). The resulting functionalized Fe_3O_4@SiO_2 was gathered by filtration followed by washing with ethanol and acetone several times and drying at 50 °C under vacuum for 12 h. The materials obtained are referred to as Fe_3O_4@SiO_2-NH_2 nanocomposite (Scheme 2).

3. 5. General Procedure for the Synthesis of 1,4-Dihydropyridine Derivatives 5a–t

A solution of aldehyde (1 mmol), malononitrile/ethylcyanoacetate (1 mmol) and Fe_3O_4@SiO_2-NH_2

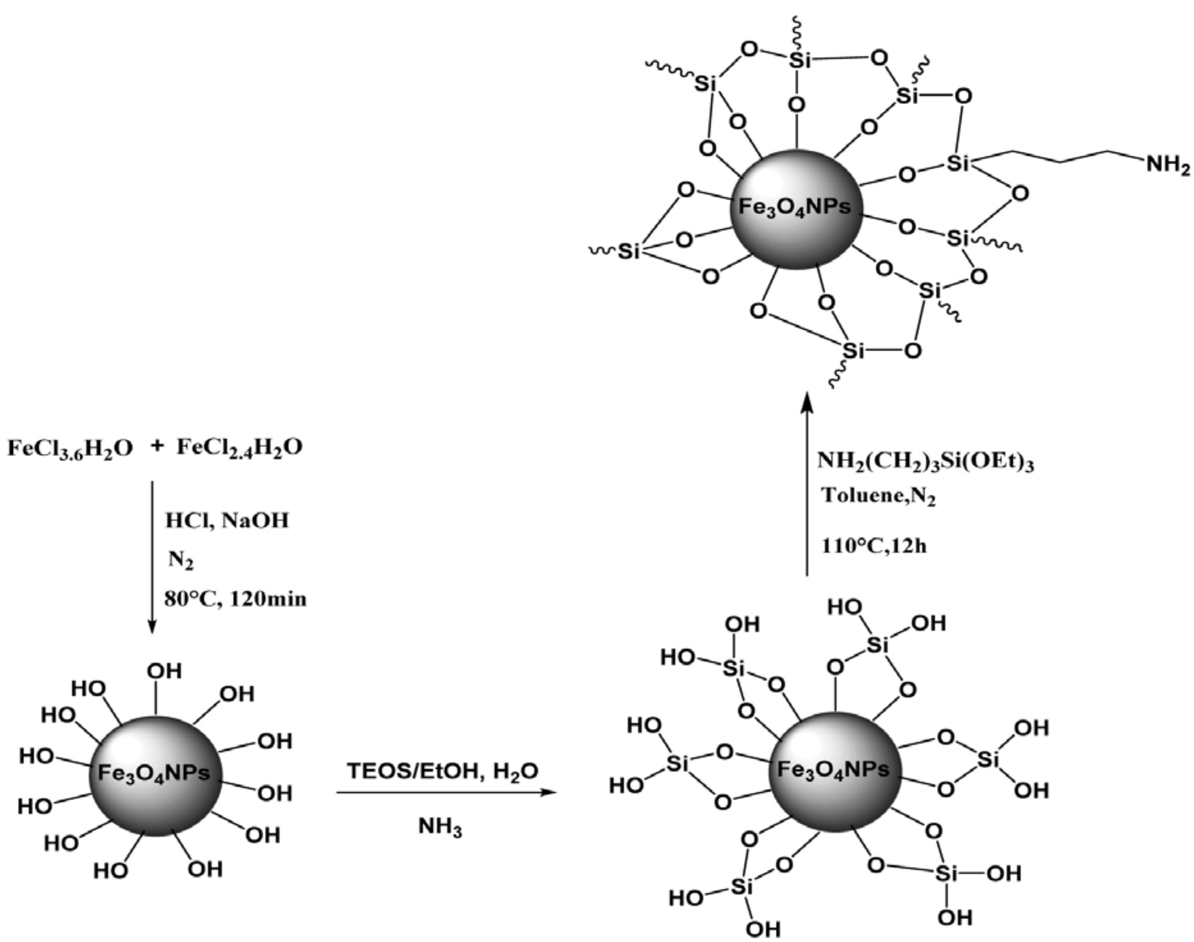

Scheme 4. Preparation of amino functionalized silica-coated magnetite nanocomposites

NPs (0.01 g) were stirred in 5 mL of ethanol at room temperature. Then, a solution of aromatic amine (1 mmol) and acetylenedicarboxylate (1 mmol) in 5 mL ethanol was added to it. The resulting mixture was stirred until the reaction was completed as indicated by thin-layer chromatography (TLC), then the catalyst was separated by an external magnet, the solid obtained was filtered and washed well with cold ethanol. The crude product was crystallized from hot ethanol to afford the pure product in high yield.

All of the products were characterized and identified with m.p., ^{1}H, ^{13}C NMR and FT-IR spectroscopy techniques. Spectral data of the new products are given below.

5-Ethyl-2,3-dimethyl-6-amino-4-(3-nitrophenyl)-1-(*p*-tolyl)-1,4-dihydropyridine-2,3,5-tricarboxylate (5m).
Yellow solid; m.p. 172–174°C; ^{1}H NMR (400 MHz, $CDCl_3$) δ 1.23 (t, 3H, CH_3), 3.46 (s, 3H, CH_3), 3.68 (s, 3H, OCH_3), 3.87 (s, 3H, OCH_3), 4.07 (q, 2H, CH_2), 5.09 (s, 1H, CH), 6.27 (2H, NH_2), 7.02 (d, 2H), 7.35 (d, 2H), 7.45 (t, 1H), 7.74 (d, 1H), 8.07 (d, 1H), 8.33 (d, 1H). ^{13}C NMR (100 MHz, $CDCl_3$) δ 14.4, 21.3, 37.2, 52.0, 52.6, 55.6, 59.6, 106.4, 121.4, 123.1, 128.8, 130.1, 130.7, 132.1, 134.0, 142.4, 148.3, 149.3, 151.6, 163.7, 165.8, 169.1. FT-IR (KBr) *ν* 3422, 3375, 3182, 2960, 2184, 1752, 1701, 1653, 1572, 1526, 1423, 1349, 1250, 1217, 1108, 1050, 970, 930, 872, 809, 783 cm^{-1}; MS (EI) *m/z* 495.16 (M$^+$); Anal. Calcd. For $C_{25}H_{25}N_3O_8$: C 60.60, H 5.09. N 8.48. Found: C 60.69, H 5.01. N 8.44.

5-Ethyl-2,3-dimethyl-6-amino-1-(4-methoxyphenyl)-4-(3-nitrophenyl)-1,4-dihydropyridine-2,3,5-tricarboxylate (5n).
Yellow solid; m.p. 178–180°C; ^{1}H NMR (400 MHz, $CDCl_3$) δ 1.23 (t, 3H, CH_3), 2.42 (s, 3H, CH_3), 3.45 (s, 3H, OCH_3), 3.64 (s, 3H, OCH_3), 4.06 (q, 2H, CH_2), 5.10 (s, 1H, CH), 6.26 (2H, NH_2), 7.27 (d, 2H), 7.32 (d, 2H), 7.46 (t, 1H), 7.72 (d, 1H), 8.05 (d, 1H), 8.33 (s, 1H). ^{13}C NMR (100 MHz, $CDCl_3$) δ 14.4, 37.2, 52.0, 52.6, 55.6, 59.5, 106.3, 115.1, 121.4, 123.0, 126.9, 128.8, 131.7, 134.0, 142.6, 148.3, 149.4, 151.8, 160.7, 163.7, 165.8, 169.1. FT-IR (KBr) *ν* 3421, 3375, 3182, 2962, 2184, 1752, 1702, 1653, 1572, 1526, 1423, 1349, 1250, 1217, 1108, 1050, 970, 930, 872, 809, 783 cm^{-1}; MS (EI) *m/z* 511.16 (M$^+$); Anal. Calcd. For $C_{25}H_{25}N_3O_9$: C 58.71, H 4.93. N 8.22. Found: C 58.83, H 4.85. N 8.19.

Dimethyl-6-amino-4-(4-chlorophenyl)-5-cyano-1-phenyl-1,4-dihydropyridine-2,3-dicarboxylate (5o).
Yellow solid; m.p. 138–140°C; ^{1}H NMR (400 MHz, $CDCl_3$) δ 3.44 (s, 3H, OCH_3), 3.60 (s, 3H, OCH_3), 4.10 (s, 2H, NH_2), 4.67 (s, 1H, CH), 7.27–7.36 (m, 6H), 7.51 (d, 3H). ^{13}C NMR (100 MHz, $CDCl_3$) δ 38.2, 52.7, 52.8, 60.9, 105.3, 120.1, 128.2, 128.5, 128.8, 129.0, 130.6, 131.2, 133.0,135.4, 137.2, 142.5, 149.1, 151.4, 163.7, 165.8. FT-IR (KBr) *ν* 3465, 3360, 3058, 2950, 2180, 1746, 1707, 1651, 1573, 1526, 1414, 1353, 1249, 1222, 1108, 1017, 971, 928, 833, 809, 784 cm^{-1}; MS (EI) *m/z* 423.10 (M$^+$); Anal. Calcd. For $C_{22}H_{18}ClN_3O_4$: C 62.34, H 4.28. N 9.91. Found: C 62.29, H 4.24. N 9. 98.

Dimethyl-6-amino-1-(4-chlorophenyl)-5-cyano-4-(4-nitrophenyl)-1,4-dihydropyridine-2,3-dicarboxylate (5p).
Yellow solid; m.p. 185–187°C; ^{1}H NMR (400 MHz, $CDCl_3$) δ 3.52 (s, 3H, OCH_3), 3.60 (s, 3H, OCH_3), 4.14 (s, 2H, NH_2), 4.81 (s, 1H, CH), 7.30 (d, 2H), 7.52 (t, 4H), 8.27 (d, 2H). ^{13}C NMR (100 MHz, $CDCl_3$) δ 20.5, 38.2, 52.7, 52.8, 61.7, 105.6, 121.9, 128.2, 128.6, 129.0, 129.3, 131.2, 131.7, 134.0, 135.6, 137.0, 141.5, 150.2, 151.8, 163.1, 168.5. FT-IR (KBr) *ν* 3449, 3354, 3055, 2951, 2186, 1744, 1710, 1651, 1575, 1519, 1421, 1346, 1229, 1226, 1111, 1014, 971, 930, 866, 823, 762 cm^{-1}; MS (EI) *m/z* 468.08 (M$^+$); Anal. Calcd. For $C_{22}H_{17}ClN_4O_6$: C 56.36, H 3.65, N 11.95. Found: C 56.39, H 3.58. N 11.90.

Dimethyl-6-amino-4-(4-chlorophenyl)-5-cyano-1-(3-nitrophenyl)-1,4-dihydropyridine-2,3-dicarboxylate (5q).
Yellow solid; m.p. 157–159°C; ^{1}H NMR (400 MHz, $CDCl_3$) δ 3.42 (s, 3H, OCH_3), 3.61 (s, 3H, OCH_3), 4.07 (s, 2H, NH_2), 4.67 (s, 1H, CH), 7.28 (d, 2H), 7.37 (d, 2H), 7.72 (s, 2H), 8.23 (s, 2H), 7.38 (d, 2H). ^{13}C NMR (100 MHz, $CDCl_3$) δ 38.1, 52.3, 53.0, 63.9, 106.2, 119.7, 125.5, 128.4, 129.1, 131.0, 133.2, 136.4, 136.5, 141.0, 142.7, 148.7, 149.1, 163.2, 165.3. FT-IR (KBr) *ν* 3454, 3346, 3054, 2952, 2182, 1741, 1714, 1650, 1573, 1525, 1420, 1346, 1227, 1225, 1118, 1014, 973, 930, 864, 823, 762 cm^{-1}; MS (EI) *m/z* 468.08 (M$^+$); Anal. Calcd. For $C_{22}H_{17}ClN_4O_6$: C 56.36, H 3.65, N 11.95. Found: C 56.31, H 3.67. N 11.97.

Dimethyl-6-amino-1-(4-chlorophenyl)-5-cyano-4-(*p*-tolyl)-1,4-dihydropyridine-2,3-dicarboxylate (5r).
Yellow solid; m.p. 191–193°C; ^{1}H NMR (400 MHz, $CDCl_3$) δ 2.35 (s, 3H, CH_3), 3.50 (s, 3H, OCH_3), 3.60 (s, 3H, OCH_3), 4.01 (s, 2H, NH_2), 4.63 (s, 1H, CH), 7.17–7.46 (m, 6H), 7.48 (d, 2H). ^{13}C NMR (100 MHz, $CDCl_3$) δ 21.1, 38.0, 52.1, 52.8, 63.7, 105.8, 120.2, 126.8, 129.6, 130.2, 131.6, 131.6, 133.7, 136.7, 136.9, 141.3, 141.6, 149.1, 163.2, 165.7. FT-IR (KBr) *ν* 3454, 3318, 3054, 2951, 2187, 1744, 1711, 1653, 1574, 1525, 1416, 1353, 1227, 1223, 1110, 1017, 972, 931, 864, 823, 762 cm^{-1}; MS (EI) *m/z* 437.11 (M$^+$); Anal. Calcd. For $C_{23}H_{20}ClN_3O_4$: C 63.09, H 4.60, N 9.60. Found: C 63.19, H 4.58. N 9.54.

Dimethyl-6-amino-5-cyano-4-(4-isopropylphenyl)-1-(*p*-tolyl)-1,4-dihydropyridine-2,3-dicarboxylate (5s).
Yellow solid; m.p. 195–197°C; ^{1}H NMR (400 MHz, $CDCl_3$) δ 1.37 (s, 9H, CH_3), 3.51 (s, 3H, OCH_3), 3.62 (s,

3H, OCH_3), 4.00 (s, 2H, NH_2), 4.64 (s, 1H, CH), 7.21–7.27 (m, 4H), 7.31 (d, 2H), 7.48 (d, 2H). ^{13}C NMR (100 MHz, $CDCl_3$) δ 23.9, 33.7, 37.9. 52.1, 52.7, 63.7, 106.0, 120.3, 126.8, 126.9, 130.2, 131.6, 133.7, 136.7, 141.2, 141.8, 147.7, 149.2, 163.5, 165.7. FT-IR (KBr) *v* 3466, 3327, 3056, 2957, 2184, 1746, 1709, 1652, 1577, 1521, 1415, 1353, 1227, 1223, 1154, 1017, 972, 929, 864, 818, 770 cm^{-1}; MS (EI) *m/z* 445.20 (M^+); Anal. Calcd. For $C_{26}H_{27}N_3O_4$: C 70.09, H 6.11, N 9.43. Found: C 70.18, H 6.04. N 9.40.

Dimethyl-6-amino-1-(4-chlorophenyl)-5-cyano-4-(4-cyanophenyl)-1,4-dihydropyridine-2,3-dicarboxylate (5t).
Yellow solid; m.p. 164–166°C; ^{1}H NMR (400 MHz, $CDCl_3$) δ 3.52 (s, 3H, OCH_3), 3.60 (s, 3H, OCH_3), 4.12 (s, 2H, NH_2), 4.74 (s, 1H, CH), 7.29 (t, 2H), 7.48 (q, 4H), 7.49 (d, 2H). ^{13}C NMR (100 MHz, $CDCl_3$) δ 38.8. 52.2, 52.9, 62.1, 104.4, 111.1, 118.7, 119.7, 127.8, 130.3, 131.5, 132.8, 133.1, 137.2, 142.2, 149.5, 163.0, 165.1. FT-IR (KBr) *v* 3467, 3337, 3059, 2951, 2185, 1746, 1709, 1652, 1575, 1521, 1415, 1353, 1227, 1223, 1152, 1017, 971, 929, 869, 820, 775 cm^{-1}; MS (EI) *m/z* 448.09 (M^+); Anal. Calcd. For $C_{23}H_{17}ClN_4O_4$: C 61.55, H 3.82, N 12.48. Found: C 61.51, H 3.86. N 12.45.

3. 6. Catalyst Recovery

After completion of the reaction, the catalyst was separated using an external magnet and then was washed three to four times with chloroform and ethyl acetate and then dried at 50 °C for 10 h. The separated catalyst was used for six cycles with a slightly decreased activity as shown in Table 4.

Table 4. Reusability of the Fe_3O_4@SiO_2-NH_2 nanocomposite

Yield (%)					
First	**Second**	**Third**	**Fourth**	**Fifth**	**Sixth**
94	93	91	90	88	87

4. Conclusions

In summary, here we describe an efficient method for the synthesis of polysubstituted dihydropyridines through a one-pot four-component reaction of aldehydes, aryl amines, dimethyl acetylenedicarboxylate and malononitrile/ethyl acetoacetate using Fe_3O_4@SiO_2-NH_2 nanocomposites at room temperature. This method offers several advantages including high yields, short reaction times, simple work-up procedure, mild and green reaction conditions, ease of separation, recyclability and reusing of the magnetic nanocatalyst.

5. Acknowledgements

The author gratefully acknowledges the financial support of this work by the Research Affairs Office of the Islamic Azad University, Qom Branch, Qom, I. R. Iran.

6. References

1. A. Kumar, R. A. Maurya, S. Sharma, M. Kumar, G. Bhatia, *Eur. J. Med. Chem*. **2010**, *45*, 501–509. http://dx.doi.org/10.1016/j.ejmech.2009.10.036
2. D. J. Triggle, D. D. Langs, R. A. Janis, *Med. Res. Rev*. **1989**, *9*, 123–180. http://dx.doi.org/10.1002/med.2610090203
3. R. P. Mason, I. T. Mak, M. W. Trumbore, P. E. Mason, *Am. J. Cardiol*. **1999**, *84*, 16–22. http://dx.doi.org/10.1016/S0002-9149(99)00360-4
4. O. Aruoma, C. Smith, R. Cecchini, P. Evans, B. Halliwell, *Biochem. Pharmacol*. **1991**, *42*, 735–743. http://dx.doi.org/10.1016/0006-2952(91)90030-9
5. M. Kawase, A. Shah, H. Gaveriya, N. Motohashi, H. Sakagami, A. Varga, *J. Bioorg. Med. Chem*. **2002**, *10*, 1051–1055. http://dx.doi.org/10.1016/S0968-0896(01)00363-7
6. C. Safak, R. Simsek, *Mini. Rev. Med. Chem*. **2006**, *6*, 747–755. http://dx.doi.org/10.2174/138955706777698606
7. M. , K. , Z. Kleinrok, R. , S. Czuczwar, **1997**, *56*, 629–635. http://dx.doi.org/10.1016/S0091-3057(96)00405-4
8. K. K. Borowicz, M. Gasior, Z. Kleinrok, S. Czuczwar, *Eur. J. Pharmacol*. **1997**, *323*, 45–51. http://dx.doi.org/10.1016/S0014-2999(97)00020-4
9. (a) D. M. Stout, *Chem. Rev*. **1982**, *82*, 223–243. http://dx.doi.org/10.1021/cr00048a004
(b) U. Eisner, J. Kuthan, *Chem. Rev*. **1972**, *72*, 1–42. http://dx.doi.org/10.1021/cr60275a001
(c) R. Lavilla, *J. Chem. Soc*. **2002**, *1*, 1141–1156.
10. M. P. S. Ishar, K. Kumar, S. Kaur, S. Kumar, N. K. Girdhar, S. Sachar, A. Marwaha, A. Kapoor, *Org. Lett*. **2001**, *3*, 2133–2136. http://dx.doi.org/10.1021/ol010026a
11. (a) M. G. Rimoli, L. Avallone, S. Zanarone, E. Abignente, A. Mangoni, *J. Heterocycl. Chem*. **2002**, *39*, 1117–1122. http://dx.doi.org/10.1002/jhet.5570390601
(b) A. Hilgeroth, A. Billich, H. Lilie, *Eur. J. Med. Chem*. **2001**, *36*, 367–374. http://dx.doi.org/10.1016/S0223-5234(01)01228-4
12. J. Sun, E. Y. Xia, Q. Wu, C. G. Yan, *Org. Lett*. **2010**, *12*, 3678–3681 http://dx.doi.org/10.1021/ol101475b
13. S. Pala, L. H. Choudhury, T. Parvin, *Synth. Commun*. **2013**, *43*, 986–992 http://dx.doi.org/10.1080/00397911.2011.618283
14. M. Hadjebi, M. S. Hashtroudi, H. R. Bijanzadeh, S. Balalaie, *Helv. Chim. Acta*. **2011**, *94*, 382–388. http://dx.doi.org/10.1002/hlca.201000228
15. B. Morak-Miodawska, K. Pluta, *Heterocycles* **2009**, *78*, 1289–1298. http://dx.doi.org/10.3987/COM-08-11622
16. E. Moreno-Manas, R. Pleixats, *Chem. Res*. **2003**, *36*, 638–643. http://dx.doi.org/10.1021/ar020267y

17. L. Mosafa, M. Moghadam, M. Shahedi, *Chin. J. Catal*., **2013**, *34*, 1897. http://dx.doi.org/10.1016/S1872-2067(12)60663-9
18. P. D. Stevens, G. Li, J. Fan, M. Yen, Y. Gao, *Chem. Commun*. **2005**, 4435–4437. http://dx.doi.org/10.1039/b505424a
19. E. Girgis, M. M. Wahsh., A. Othman, J. L. Bandhu, K. V. Rao, *Nano. Res. Lett*. **2011**, *6*, 460–466. http://dx.doi.org/10.1186/1556-276X-6-460
20. F. Nemati, M. M. Heravi., R. Saeedi Rad, *Chin. J. Catal*. **2012**, *33*, 1825–1831. http://dx.doi.org/10.1016/S1872-2067(11)60455-5
21. Q. Du, W. Zhang, H. Ma, J. Zheng, B. Zhou, Y. Li, *Tetrahedron* **2012**, *68,* 3577–3584. http://dx.doi.org/10.1016/j.tet.2012.03.008
22. H. Yang, S. Li, X. Wang, F. Zhang, X. Zhong, Z. Dong. J. Ma, *J. Mol. Catal. A-Chem*. **2012**, *363–364*, 404–410. http://dx.doi.org/10.1016/j.molcata.2012.07.017
23. W. Li, B. Zhang, X. Li, H. Zhang, Q. Zhang, *Appl. Catal. A-Gen*. **2013**, *459*, 65–72. http://dx.doi.org/10.1016/j.apcata.2013.04.010
24. A. Hu, G. T. Yee, W. Lin, *J. Am. Chem. Soc*. **2005**, *127*, 12486–12487. http://dx.doi.org/10.1021/ja053881o
25. P. Wang, A. Kong, W. Wang, H.Y. Zhu, Y. K. Shan, *Catal. Lett*. **2010**, *135*, 159–164. http://dx.doi.org/10.1007/s10562-010-0271-x
26. F. Zamani, S. Kianpour, *Catal. Commun*. **2014**, *45*, 1–6. http://dx.doi.org/10.1016/j.catcom.2013.10.027
27. B. Atashkar, A. Rostami, B. Tahmasbi, *Catal. Sci. Technol*. **2013**, *3*, 2140–2146. http://dx.doi.org/10.1039/c3cy00190c
28. A. Alizadeh, M. M. Khodaei, M. Beygzadeh, D. Kordestani, M. Feyzi, *Bull. Korean Chem. Soc*. **2012**, *33*, 2546–2552. http://dx.doi.org/10.5012/bkcs.2012.33.8.2546
29. T. Zeng, L. Yang, R. Hudson, G. Song, A. R. Moores, C. Li, *Org. Lett*. **2011**, *13*, 442–445. http://dx.doi.org/10.1021/ol102759w
30. M. A. Ghasemzadeh, J. Safaei-Ghomi, H. Molaei, *C. R. Chimie*. **2012**, *15*, 969–974. http://dx.doi.org/10.1016/j.crci.2012.08.010
31. M. A. Ghasemzadeh, J. Safaei-Ghomi, *Acta. Chim. Slov*. **2015**, *62*, 103–110.
32. M. A. Ghasemzadeh, J. Safaei-Ghomi, S. Zahedi, *J. Serb. Chem. Soc*. **2013**, *78*, 769–779.
33. M. A. Ghasemzadeh, J. Safaei-Ghomi, *J. Chem. Res*. **2014**, *5*, 313–316. http://dx.doi.org/10.3184/174751914X13976454726953
34. M. A. Ghasemzadeh, *Acta. Chim. Slov*. **2015**, *62,* 977–985. http://dx.doi.org/10.17344/acsi.2015.1501
35. Y. Hu, Z. Zhang, H. Zhang, L. Luo, S. Yao, *J. Solid State Electro. Chem*. **2012**, *16*, 857–867. http://dx.doi.org/10.1007/s10008-011-1434-4
36. Y. H. Deng, D. W. Qi, C. H. Deng, X. M. Zhang, D. Y. Zhao, *J. Am. Chem. Soc*. **2008**, *130*, 28–29. http://dx.doi.org/10.1021/ja0777584
37. J. Wang, S. Zheng, Y. Shao, J. Liu, Z. Xu, D. Zhu, *J. Colloid Interface Sci*. **2010**, *349*, 293–299. http://dx.doi.org/10.1016/j.jcis.2010.05.010

Povzetek

Opisujemo praktično, enostavno in učinkovito metodo za sintezo polisubstituiranih dihidropiridinov s pomočjo večkomponentne reakcije med aldehidi, arilamini, dimetil acetilendikarboksilatom in malononitrilom/etil acetoacetatom v prisotnosti Fe_3O_4@SiO_2-NH_2 nanokompozitov. Predstavljena metodologija je nov in učinkovit način sinteze dihidropiridinskih derivatov, ki prinaša kar nekaj prednosti: odlične izkoristke, kratke reakcijske čase, ponovno uporabo in majhno potrebno množino katalizatorja. Nanomagnetni katalizator lahko namreč po reakciji zlahka izoliramo z uporabo zunanjega magneta in uporabimo večkrat brez posebne izgube učinkovitosti. Katalizator smo popolnoma karakterizirali z analizami FT-IR, SEM, XRD, EDX in VSM.